Using aqueous foams to synthesize cadmium sulfide nanoclusters

Mrs. Usha Raghavan
Head of Information Technology,
V.P.M's Polytechnic,Thane
Email-id: - usharagha@gmail.com

Abstract

Surfactant based aqueous foams provide a very efficient and simple chemical route for the synthesis of various nanomaterials with controllable structure, size and shape. In this present work, a one-step process for the synthesis of morphologically controlled CdS nanoclusters has been described. Aqueous soluble $CdCl_2$ and the surfactant AOT are homogeneously mixed together to produce a stable aqueous foam. Once all the water content is drained, the freestanding dry foam containing the cadmium salt is treated with H_2S vapor. This sulphidation procedure of the completely dried foams yields CdS nanoclusters of variable morphology. TEM and XRD measurements confirm the particle size to be less than 10 nm. The optical absorption spectra clearly show a well defined exciton absorption feature around 450 nm due to quantum confinement effects. The interesting emission characteristics of the as-prepared AOT-capped CdS nanoparticles were discussed with respect to their size and shape.

Keywords: *Aqueous Foams, Aerosol-OT, CdS Nanoclusters, Alloyed CdMnS Nanocrystals,Zincblende, Quantum Confinement, Absorption and Fluorescence*.

Author is doing research in Nanotechnology under the guidance of Dr.Murali Sastry in Pune University.

Introduction

The synthesis of inorganic semiconductor nanocrystals in a controllable fashion, with their exciting size and shape dependent electronic and optical properties has been the goal of much active research over the past decade as they provide information about the evolution of physical characteristics from atom to bulk and about the three-dimensional confinement of carriers and excitons.[1-5] Among other semiconductors, CdS nanoparticles stand alone having potential applications as optoelectronic devices,[6] lasers,[7] photocatalysts,[8] electrochemical cells,[9] molecular recognition and neurotransmitters,[10] fluorescent markers for biological labeling[11] etc. These exciting applications have focused attention on the synthesis, size control and organization of CdS nanoclusters.[4,12-13]

Till now, all the available semiconductor nanoparticle preparations focus mainly on the size, shape and surface uniformity, which greatly improves their spectroscopic characterization.[1,3-4,12-13] Also, surface passivation reduces surface effects, enhancing the exciton effects.[5] The surface sensitivity of the confined exciton has resulted in great emphasis on the synthesis procedures, which led to the enormous progress in the preparation of more sharply distributed samples with controlled surface structures.[2,4,12-13] The improved synthesis results from different approaches such as wet chemical routes,[14] organometallic precursor based synthesis procedures,[15] ion-entrapment process,[16] biosynthesis,[17] electrochemical,[12] reversed micelles,[18] vesicles, Langmuir Blodgett films,[19] and sol gel.[20] Aqueous surfactant based synthesis procedure is being employed in the present work.

Until now, water based synthesis protocols were scarcely utilized to control the shape characteristics of CdS nanoparticles. We address this particular lacuna in the present work and describe a simple ambient temperature process for the synthesis of CdS nanocrystals with high shape anisotropy as well as ones that are nearly spherical, by simply adjusting the environment of the surfactant. Surfactant-assisted methods have already been widely used in the preparation and morphology control of inorganic nanomaterials, particularly the semiconductors.[18] The surfactant-covered water pools (or reversed micelles as they are commonly called) offer a unique microenvironment for the formation of nanoparticles by not only serving as microreactors for processing the reactions but also inhibiting the excess aggregation of particles. The size of the nanoparticle is restricted by the size of the microaqeuous core of the reversed micelle in which it is formed, with polydispersity values usually in the range of 10-15%. The use of functional surfactants allows, by blocking one of the reactants at the interface of the micelles, semiconductor colloids to be obtained that are more stable and smaller than those obtained from ions solubilized in the water pool of the reversed micelle.[18]

Earlier, synthesis of semiconductor nanoparticles is generally achieved by mixing water in oil microemulsions containing the appropriate reactants within the reversed micelles.[18] Many metal sulphide nanoparticles have been synthesized in this way by mixing two w/o microemulsions containing the suitable water-soluble metal salt and sodium sulphide, respectively.[18] A disadvantage of this procedure arises if the use of the nanoparticles requires their separation from the reaction medium. Bare nanoparticles are thermodynamically unstable with respect to growth and, after extraction, they tend to spontaneously coalesce loosing their peculiar properties.

The present approach of aqueous surfactant based foam synthesis of nanoparticles seems to be a promising one as the micro heterostructure of the foam itself acts as ideal nanosized reactors to synthesize as well as to host a wealth of nanoparticles. In general, foams provide a high surface area of gas bubbles dispersed in a liquid.[21] The stabilizing surfactant or other amphiphile adsorbed at the gas/liquid interface offers greater possibility for the use of liquid lamellae as a plausible template for growing wide variety of inorganic materials. Since the thickness of the liquid lamellae is controlled by the drainage within the plateau borders of the foam, it also follows that the size of the resulting inorganic crystals may be controlled via the drainage rate.[21]

The choice of the surfactant, sodium bis(2-ethylhexyl)sulfosuccinate (AOT), was motivated by the possibility of better size control over formation of CdS nanoparticles.[18] AOT, a well-known capping agent for semiconductor nanoparticles, is a double chain anionic surfactant. AOT reversed micelles have been widely used as nanoreactors and nanocontainers because their structural and dynamical properties are well established.[18] It has been found that the size and concentration of AOT reversed micelles strongly influence the structural and photophysical properties of synthesized nanoparticles. In particular, it is well known that AOT reversed micelles are nearly spherical and has a surfactant packing parameter, *P*, of 1.1 (*P*) V/*al*, where V is the volume occupied by the tails, *a* the effective head group cross-sectional area, and *l* the maximum effective tail length). The surfactant thus tends to have a spontaneous curvature that is concave toward water, leading to the formation of spherical reversed micelles above the critical micelle concentration (CMC).[18]

AOT reversed micelles not only make possible the in situ synthesis of very small particles but also used as the structure directing agent in synthesizing CdS nanoparticles of various morphologies. Electrostatic interactions help the cadmium ions to bind with the anionic surfactant molecules during the foam formation stage itself. Subsequently, the aqueous drained dry foams, when treated with H_2S vapors yields CdS nanoparticles of various sizes depending on the bubble size of the foam as well as the vapor content. A highlight of this study is our observation that CdS nanoparticles of variable morphology are formed within different regions of the foam. We believe this is due to the variation in structure across the foam that presents reaction cavities of variable thickness. Presented below are the details of the investigation.

Experimental Details

Chemicals. Cadmium Chloride, $CdCl_2$ and sodium bis(2-ethylhexyl)sulfosuccinate (AOT) were obtained from Aldrich Chemicals and used as-received.

Preparation of CdS nanocrystals in aqueous AOT foam

In a typical experiment, a rectangular column of 50 cm height and a square base of 10 x 10 cm^2 with sintered ceramic discs embedded in it were used for generation of the foam. An aqueous mixture of 100 ml of 10^{-2} M cadmium chloride and 100 ml of 10^{-2} M AOT were taken in the rectangular column and the foam was built up by injecting air at a pressure of 1-5 psi through a porous ceramic disc fixed to the bottom of the foam column. Stable foams up to 40 cm height and with bubble size of 1 mm could routinely be obtained. After carefully draining out the excess aqueous AOT + $CdCl_2$ solution, the whole column containing the cadmium ions within the dry foam were subjected to H_2S vapors. As the vapor passes through the interfaces in the dry foam column slowly but

steadily, the entire column slowly but steadily changes to yellowish orange color indicating the formation of the CdS nanoparticles. Once the CdS formation completes, the foam column gradually starts collapsing and the resulting solution could easily be collected for further analysis. This solution (sample 1) was then subjected to centrifugation at 5000 rpm for 30 minutes following which the pellet (sample 2) and supernatant (sample 3) were separated and characterized by different techniques. Please note that sample 2, for further analysis, was prepared by redispersing and sonicating the CdS nanoparticle pellet in 10 ml of water.

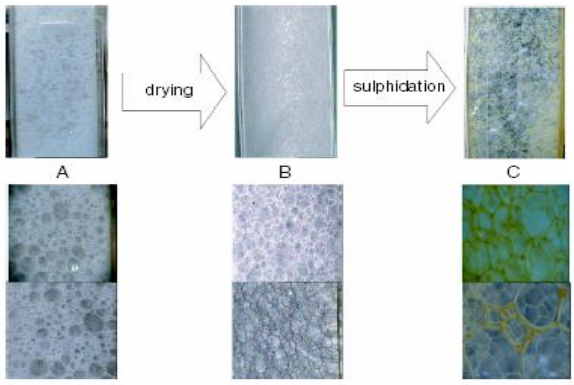

Scheme 1. Foam column (top) and the corresponding magnified bubble images (bottom) analyzed during different stages of CdS nanoparticles formation clearly illustrates the role of Plateau border regions in the foam. (A) Wet foam with small spherical bubbles formed by slow bubbling of N_2 gas into the aqueous AOT + $CdCl_2$ mixture, (B) The stable dry foam with polyhedral honey-comb like structures after 3 hours of drainage and (C) Formation of CdS nanoparticles along the Plateau borders after complete reaction with H_2S gas (see text for details).

UV-vis spectroscopic studies

The optical properties of the AOT-capped CdS nanoparticle solutions, sample **1**, **2** and **3** were monitored on a JASCO model V-570 diode array spectrophotometer operated at a resolution of 2 nm in the UV-visible region of 200-800 nm.

Fluorescence studies

The photoluminescence/fluorescence measurements of the AOT-capped nanoparticle solutions were done on a Perkin Elmer model LS 50-B spectrofluorimeter at 25°C, with slit widths of 5 nm for excitation at 420 nm and 10 nm for the emission monochromators.

X-ray diffraction measurements

X-ray diffraction (XRD) analysis of the drop-coated films on glass substrates from the AOT-capped CdS nanoparticles was carried out on a Phillips PW 1830 instrument operating at 40 kV and a current of 30 mA with Cu K_α radiation.

Transmission Electron Microscopy (TEM) measurements

TEM measurements were performed on a JEOL model 1200EX instrument operated at an accelerating voltage at 120kV. Samples for TEM studies were prepared by placing drops of the AOT-capped CdS nanoparticles in samples **1**, **2** and **3** on carbon-coated TEM grids. The films on the TEM grids were allowed to dry for 2 min following which the extra solution was removed using a blotting paper.

Results and Discussion

Fig. 1A illustrates the UV-visible spectra of the AOT-capped CdS nanoparticles corresponding to the as-prepared foam solution (curve 1), redispersed pellet (curve 2) and the supernatant (curve 3) respectively.

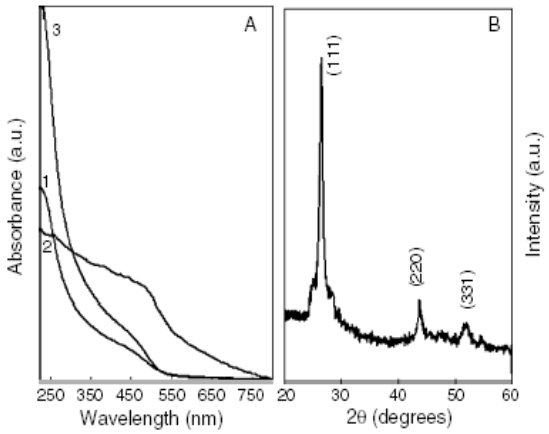

Fig. 1. (A) UV-visible absorption spectra of the CdS nanoparticles obtained from the foam (**1**, curve 1), the CdS nanoparticles after centrifugation and redispersion (**2**, curve 2) and the supernatant after centrifugation (**3**, curve 3). (B) XRD pattern of the drop coated film on a glass substrate from the CdS pellet solution after centrifugation. The Bragg reflections from CdS nanoparticles are indexed as shown (text for details).

The inset figure shows the corresponding CdS nanoparticle solutions. The yellowish orange colors of these solutions indicate the formation of the CdS nanoparticles. The characteristic excitonic peak centered on 450 nm clearly reveals the quantum confinement effect arising due to the smaller size of the as-formed CdS nanoparticles. The size of the nanoclusters corresponding to the absorption onset as shown in fig. 1A is in good agreement with the size determined from XRD and TEM measurements as discussed below. The stability of these solutions even after few months of storage clearly indicates that the aggregation of particles were restrained by the strong surface binding of the surfactant AOT molecules with the CdS nanoparticles. Fig. 1B depicts the crystalline XRD pattern of the AOT-capped CdS nanoparticles. The Bragg reflections, as illustrated, indicate the formation of the stable wurtzite structure of CdS. All the three samples show the similar XRD patterns and thus have not been shown for brevity.

Fig. 2 shows the TEM micrographs of lower and higher magnifications for the as-prepared CdS nanoparticles from the dry foam. The ribbon-like CdS structures capped with AOT are clearly seen in figs. 2A and B. The corresponding selected area electron diffraction pattern shown as the inset reveals the crystalline nature of the as-formed CdS nanoparticles. This diffraction pattern corresponds to the hexagonal structure of CdS in accordance with the XRD measurements as shown in fig. 1B.

Centrifugation of these as-prepared AOT-capped CdS nanoparticles retain a purified pellet, free from any uncoordinated surfactant molecules and also a supernatant solution which contains the uncapped dispersed CdS nanoparticles.

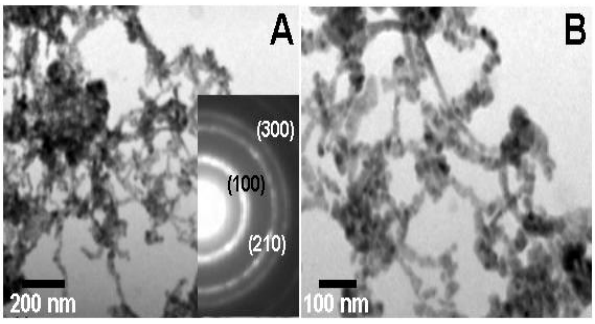

Figure 2. Representative TEM micrographs recorded at different magnifications from the drop cast films of AOT capped CdS nanoparticles as-prepared in the foam column. The inset in figure B shows the selected area electron diffraction (SAED) for the dense ribbon-like CdS nanostructures.

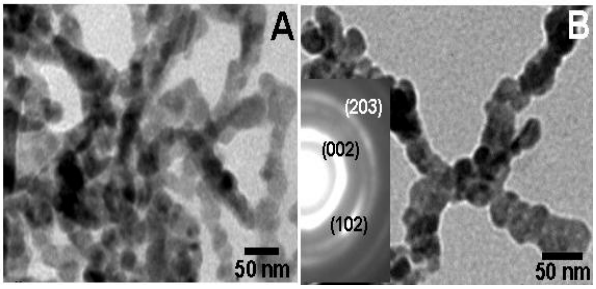

Figure 3. Representative TEM micrographs recorded at different magnifications from the drop cast films of AOT capped CdS nanoparticles as-prepared from the centrifuged pellets, which are redispersed and sonicated in aqueous solution. The dense flat and twinned ribbon like CdS nanostructures clearly indicates the strong binding of AOT with CdS during the preparation procedure itself (see text for details). The inset in figure B shows the selected area electron diffraction (SAED) for the dense ribbon-like CdS nanostructures.

Fig. 3 shows the lower and higher magnification TEM micrographs of the CdS pellet redispersed and sonicated in aqueous solution. The highly dense, twinned ribbon-like structures clearly points out the strong surface binding of the AOT molecules with the CdS nanoparticles, thereby restricting their aggregation by ostwald ripening even in

aqueous solution. Interestingly, the redispersed solution is very stable for few months, thereby illustrating the novelty of our aqueous foam based synthesis of nanoparticles.

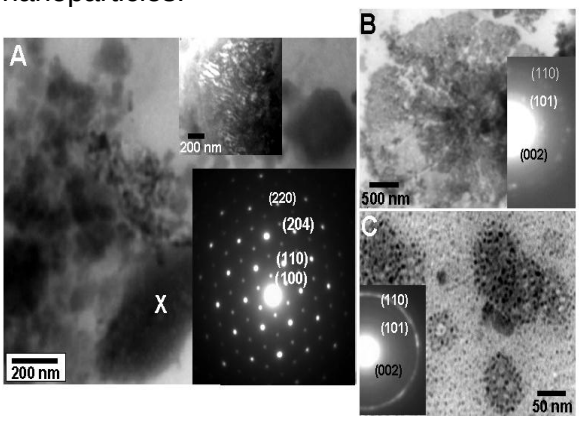

Figure 4. Representative TEM micrographs recorded at different positions from the drop cast films of AOT capped CdS nanoparticles present in the supernatant solution. These uncapped CdS nanoparticles show various interesting morphologies as follows. (A) In the supernatant solution, some of the CdS nanoparticles assembled themselves in honey-comb like structures (marked **X**) and are single crystalline in nature. The corresponding dark field image and the SAED pattern are shown as the inset figures. (B) CdS nanoparticles also assemble into flower/plate like structures as shown and its SAED pattern is given as inset. (C) As expected for the usage of AOT molecules, spherical CdS clusters were also seen and its SAED pattern as inset. (See text for further details).

Fig. 4 shows the TEM micrographs of the CdS nanoparticles present in the supernatant solution. To our surprise, spherical nanoparticles with variable morphologies have been found to be uniformly disturbed throughout the supernatant solution. In general, the supernatant solutions obtained by centrifugation contain only the uncapped particles. In the present case, the CdS nanoparticles were compressed to form monolayer like honey-comb like structures (figure 4A). The dark field image (inset in figure 4A) confirms the presence of CdS nanoparticles in these structures, which produce single crystalline like diffraction spots (inset in figure 4A) instead of the usual diffraction arches. These fascinating structures might have formed as a result of the dense random twinned structures observed in the foam and the centrifuged pellet. This interesting variation in CdS nanoparticle morphology along with a possible change in crystal structure is an interesting example of surfactant templating of nanoparticle morphology during synthesis procedure itself. It is worth pursuing the detailed structural analysis of these nanoparticles and their mechanism of formation also. This is an interesting observation as opposed to the fact that in typical AOT reversed micelles, the CdS nanoparticles obtained were spherical in shape and relatively monodisperse in terms of size.[18] It is speculated that this change in morphology can be related to the shape of the reversed micelle in which the CdS was synthesized, and may be the direct evidence for surfactant templating. Flower/plate like CdS nanostructures were also seen which polycrystalline in nature (figure 4B). Finally, as expected from the AOT based synthesis procedure for semiconductor nanoparticles,[18] uniform distribution of polycrystalline spherical clusters of CdS nanoparticles was also seen (figure 4C).

The morphology of the CdS nanoparticles varies from spherical to flat ribbon like structures and simple centrifugation enables separation of these different shapes. This morphology control is believed to occur due to differences in the structure of the foam which varies from highly anisotropic (liquid lamellae between bubbles) to extended and isotropic (junction between plateau borders).[21] A combination of extremely large interfacial templating area provided by the liquid lamellae in foams and

the dynamic nature of the foam bubbles makes this method potentially exciting for the large-scale synthesis of other inorganic materials (nanomaterials) and minerals and are currently being attempted in our group.[22]

To further quantify the formation of CdS nanoparticles, emission spectra of all the samples were recorded at an excitation wavelength of 420 nm (fig. 5). The characteristic emission observed for our CdS nanoparticles lies in the visible region of 450 - 600 nm. In all the three samples, the peak at 480 nm corresponds to the band gap or near band gap emission resulting from the recombination of the electron-hole pair and the broader band at 530 nm is assigned to deeply trapping surface states (as it occurs at a much lower energy relative to the absorption band edge), which originates from the trapped charge carrier recombination due to surface defects.[18b] In the as-prepared CdS nanoparticles in foam (curve 1), the presence of large fraction of the surfactant AOT molecules quenches the fluorescence emission to a considerable extent, as clearly seen by the damping of the exciton emission at 480 nm. In this case, as no delocalized emission is possible, emission due to the surface states at around 530 nm dominates. In the case of the redispersed pellet, the 480 nm exciton emission clearly dominates (curve 2) indicating that uncoordinated AOT molecules are removed by centrifugation. Purified samples of these CdS nanoparticles are very stable and easily dispersed in other solvents and polymers for future applications in displays and switching devices. Further in the supernatant also, the exciton emission is considerably increased (curve 3).

It is also to be remembered that the semiconductor nanocrystals trapped in aqueous AOT reversed micelles exhibit longer excited state lifetimes (about 10-100 ns) than those present in organic solvents.[23] Clearly, the nanoparticle-surfactant interaction is not only important in restricting the growth but also in extending the lifetime of the excited states.[24]

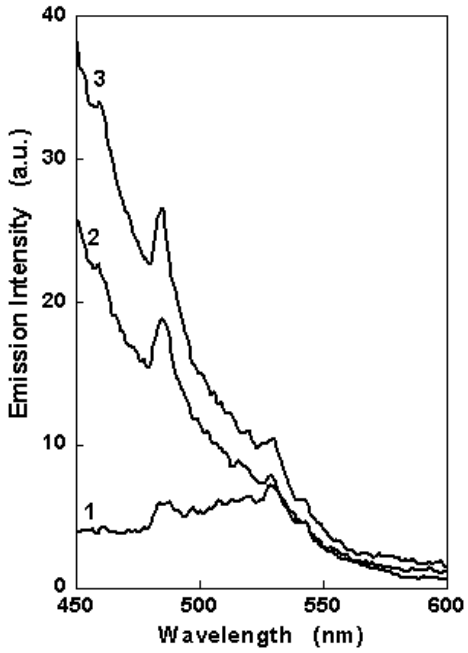

Figure 5. Fluorescence emission spectra for the AOT-capped CdS nanoparticles (excitation wavelength is 420 nm) obtained from foam (curve 1), redispersed pellet (curve 2) and the supernatant (curve 3).

In the steady state fluorescence spectra of the CdS nanoparticles synthesized in foam (curve 1, figure 5), the deep trap emission occurring at 530 nm allows for the trapping of the electrons and holes at the surface-trap sites nonradiatively and gives the low-energy trap emission usually with low quantum yield. The presence of excess water molecules on the surface of the nanoparticles would also account for the observed reduced emission, which could eventually be removed by centrifugation.[24] The chemical environment provided by the sulfate AOT reversed micelle also leads to greater surface-state emission relative to aqueous suspensions due to the small water volume. It is important to mention that the polar groups of surfactant molecules in the AOT reversed micelle seem to contribute to carrier trapping and recombination with reduced nonradiative

probability. This enhanced deep-trap emission in reversed micellular systems may be useful in the study of electronic-state decay and electron transfer processes in nanoparticles with surface acceptors. The exact nature physical and chemical of the surface-trapping sites depends on the type of nanoparticles, the capping materials, and the surrounding solvent[18] as well as the preparative technique itself.[25]

The quenching of exciton emission, the occurrence of surface-state emission, and the large Stokes shift observed in the case of aqueous foam synthesized AOT-capped CdS nanoparticles (curve 1, fig. 5) suggest very efficient energy dissipation during the exciton relaxation. It is well known that there are two ways of carrier motion — ballistic and phonon-assisted. The elimination of such efficient energy dissipation via phonons is the basis of efficient exciton emission in semiconductor nanoparticles. In general, the surface states result from defects, dangling bonds, and polar adsorbates. In the absence of any inorganic capping, there is no carrier confinement because these surface states may efficiently couple with the exciton states via interfacial phonons. The result of this efficient coupling is the loss of exciton emission and the appearance of the deep-trap emission.[18b,24]

Recently, the role of both organic and inorganic impurities in enhancing and quenching the fluorescence has been emphasized for various semiconductor nanoparticles.[26,27] Thus, from the analysis of our present emission spectra, it can be inferred that the quenching of the fluorescence can be lowered by increasing the cadmium concentration. The reason for this can be that for excess concentration of Cd^{2+}, the number of traps generated on the surface is increased, decreasing the probability of encounter of the quencher molecule with the electrons for a given quencher concentration. Since water is the working solvent in our present synthesis procedure, the study of effect of surfactants on these systems is then of remarkable importance, as they can alter the nature of behavior of the charge carriers at the surface traps.

In summary, the formation of CdS nanoparticles stabilized by the surfactant AOT in aqueous foam has been described. The process of cadmium entrapment with the surfactant in the foam completely differs from that of the conventional micellular synthesis procedures and on exposure to H_2S vapors results in the formation of CdS nanostructures with various fascinating morphologies. Simple centrifugation helps in separating different shaped CdS nanoparticles. This morphology control could as well be controlled to certain extent by varying the foam bubble size, the metal precursor and the amount of vapor content which is currently under progress. In an attempt to increase the quantum yield of the as-prepared semiconductor nanoparticles, doping strategies are also being carried out. A combination of extremely large interfacial templating area provided by the liquid lamellae in foams and the dynamic nature of the foam bubbles makes this method potentially exciting for the large-scale synthesis of other inorganic materials (nanomaterials) and minerals and are currently being attempted.

Acknowledgments

One of the authors (PSK) acknowledges the Council of Scientific and Industrial Research (CSIR, India) for the award of Research Associateship.

References

1. A. Henglein, Chem. Rev., **1989**, *89*, 1861.
2. (a) A.P. Alivisatos, *J. Phys. Chem*. **1996**, *100*, 13226. (b) Alivisatos, A. P. *Science* **1996**, *271*, 933.
3. (a) H. Weller, Angew. Chem., Int. Ed. Engl., **1993**, *32*, 41. (b) Y. Wang, Acc. Chem. Res., **1991**, *24*, 133.
4. (a) Mark Green and Paul O"Brien, Chem. Comm. **1999**, 2235. (b) T. Trindade, Paul O"Brien and N.L. Pickett, Chem. Mat. **2001**, *13*, 3843.
5. (a) Yoffe, A. D. *Adv. Phys*. **2000**, *50*, 1. (b) R.F. Khairutdinov, Russ. Chem. Rev. ***1998***, *67*, 109
6. (a) V. L. Colvin, M. C. Schlamp and A. P. Alivisatos, Nature, **1994**, *370*, 354. (b) B. O. Dabbousi, M. G. Bawendi and O. Onitsuka, Appl. Phys. Lett., **1995**, *66*, 1316.
7. L. Pavesi, L. D. Negro, C. Mazzoleni, G. Franzo and F. Priolo, Nature, **2000**, *408*, 440.
8. C. K. Gratzel and M. Gratzel, J. Am. Chem. Soc., **1979**, *101*, 7741.
9. (a) A. Hagfeldt and M. Gratzel, Chem. Rev., **1995**, *95*, 49. (b) Ningning Zhu, Aiping Zhang, Pingang He and Yuzhi Fang, *Analyst*, **2003**, *128*, 260.
10. (a) Jessica O. Winter, Timothy Y. Liu, Brian A. Korgel and Christine E. Schmidt, Adv. Mat. **2001**, *13*, 1673. (b) Cheng-Yu Lai, B.G. Treqyn, D.M. Jeftinija, K. Jeftinija, S. Xu, S. Jeftinija and Victor S.Y. Lin, J. Am. Chem. Soc. X. Michalet, F. Pinaud, T.D. Lacoste, M. Dahan, M.P. Bruchez, A. Paul Alivisatos and S. Weiss, Single Mol., **2001**, *2*, 261.
11. R.M. Penner, *Acc. Chem. Res*. **2000**, *33*, 78.
12. (a) Chung-Sung Yang, David D. Awschalom, and Galen D. Stucky, *Chem. Mater.* **2002,** *14*, 1277. (b) Zheng-Ping Qiao, Gang Xie, Jun Tao, Zhao-Yang Nie, Yan-Zhi Lin, and Xiao-Ming hen, J. Solid State Chem. ***2002***, *166*, 49. (c) E. Caponetti, L. Pedone, D. Chillura Martino, V. Panto and V. Turco Liveri, Mat. Sci. Eng. C **2003**, *23*, 531.
13. Kei Murakoshi, Hiroji Hosokawa, Miwa Saitoh, Yuji Wada, Takao Sakata, Hirotaro Mori, Mitsunobu Satoh, and Shozo Yanagida, J. Chem. Soc., Faraday Trans., ***1998***, 94, 579.
14. Yunchao Li, Xiaohong Li, Chunhe Yang and Yongfang Li, J. Mater. Chem. **2003**, *13*, 2641.
15. (a) S. Mandal, C. Damle, S.R. Sainkar and Murali Sastry, *J. Nanosci. Nanotech.* **2001**, *1*, 281. (b) S. Shiv Shankar and Murali Sastry, *PhysChemComm.* **2003**, *6***,** 36.
16. (a) P. Williams, E. Keshavarz-Moore and P. Dunnill, J. Biotech. **1996**, *48*, 259. (b) W. Shenton, D. Pum, U.B. Sleytr and S. Mann, Nature, ***1997***, *389*, 585. (c) A. Ahmad, P. Mukherjee, D. Mandal, A. Khan, S. Senapati, M.I. Khan, R. Kumar and Murali Sastry, **2002**, *124*, 12108. (d) Gioacchino Scarano and Elisabetta Morelli, Plant Science, ***2003***, *165*, 803. (e) Daisuke Ishii, Kazushi Kinbara, Yasuhiro Ishida, Noriyuki Ishii, Mina Okochi, Masafumi Yohda and Takuzo Aida, Nature, **2003**, *423*, 628.
17. (a) C. Petit, P. Lixon and M.P. Pileni, J. Phys. Chem. ***1990***, *94*, 1598. (b) B. S. Zou, R. B. Little, J. P. Wang, M. A. El-Sayed, Int. J. Quant. Chem. ***1999***, *72*, 439. (c) Blake A. Simmons, Sichu Li, Vijay T. John, Gary L. McPherson, Arijit Bose, Weilie Zhou and Jibao He, Nano Lett. ***2002***, *2*, 263.
18. (a) Jian Jin, Lin Song Li, Yan Qing Tian, Yan Jie Zhang, Yang Liu, Ying Ying Zhao, Tong Shun Shi, Tie Jin Li, Thin Solid Films, ***1998***, *327-329*, 559. (b) Chinmay Damle, A. Gole and Murali Sastry, *J. Mater. Chem.* **2000**, *10*, 1389.
19. Jian Yang, Jing-Hui Zeng, Shu-Hong Yu, Li Yang, Gui-en Zhou and Yi-tai Qian, *Chem. Mater.* **2000,** *12*, 3259. (b) Meng Chen, Yi Xie, Jun Lu, Yujie Xiong, Shuyuan Zhang, Yitai Qian and Xianming Liu, J. Mater. Chem., ***2002***, *12*, 748.
20. (a) D.L. Weaire and S. Hutzler in *Mechanics for a New Millennium* edited by H. Aref and J.W. Philips, Kluwer Academic Publishers, The Netherlands, **2001**, 275. (b) D.L. Weaire, S. Hutzler, S. Cox, N. Kern, M.D. Alonso and W. Drenckhan, J. Phys. Condens. Matter, **2003**, *15*, S65. (c) W. Drenckhan, F. Elias, S. Hutzler, D. Weaire, E. Janiaud and A.C. Bacri, Appl. Phys. Lett. **2003**, *93*, XXXXX.
21. Saikat Mandal, Sujatha K. Arumugam, Suguna D. Adyanthaya, Renu Pasricha and Murali Sastry, J. Mat. Chem. **2003**, (In press).
22. M. Hamity_, R.H. Lema, C.A. Suchetti, J. Photochem. Photobiol. A: Chem. ***2000***, *133*, 205.
23. M. Tata, S. Banerjee, V.T. John, Y. Waguespack and G.L. McPherson, Coll. Surf. A: Physiochem. Eng. Asp. ***1997***, *127*, 39.
24. J.Aquilar-Hernandez, G. Contreras-Puente, A. Morales-Acevedo, O. Vigil-Galan, F.Cruz-Gandarilla, J. Vidal-Larramendi, A. Escamilla-Esquivel, H. Hernandez-Contreras, M. Hesiquio-Garduno, A. Arias-Carbajal, M. Chavarria-Castandea and G. Arriaga-Mejia, Semicond. Sci. Technol. **2003**, *18*, 111.
25. (a) C.F. Landes, C. Burda, M. Braun, and M.A. El-Sayed, *J. Phys. Chem. B* ***2001***, *105,* 2981. (b) C.F. Landes, M. Braun and M.A. El-Sayed, *J. Phys. Chem. B* ***2001***, *105,* 10554.
26. P. Senthil Kumar and C.S. Sunandana, NanoLett. ***2002***, *2*, 975.